Deformation effect in the fast neutron total cross section of aligned ^{59}Co

U. Fasoli, P. Pavan, D. Toniolo, G. Zago, and R. Zannoni
Istituto di Fisica dell'Università degli Studi, 35100 Padova, Italy
and Istituto Nazionale di Fisica Nucleare, Sezione di Padova, 35020 Legnaro, Italy

G. Galeazzi
Istituto Nazionale di Fisica Nucleare, Laboratori di Legnaro, 35100 Padova, Italy
(Received 26 July 1982)

The variation of the total neutron cross section, $\Delta\sigma_{\text{align}}$, on ^{59}Co due to nuclear alignment of the target has been measured over the energy range from 0.8 to 20 MeV employing a cobalt single crystal with a 34% nuclear alignment. The results show that $\Delta\sigma_{\text{align}}$ oscillates from a minimum of -5% at about 2.5 MeV to a maximum of $+1\%$ at about 10 MeV. The data were successfully fitted by optical model coupled-channel calculations. The coupling terms were deduced from a model representing the ^{59}Co nucleus as a vibrational ^{60}Ni core coupled to a proton hole in a $(1f_{7/2})$ shell, without free parameters. The optical model parameters were determined by fitting the total cross section, which was independently measured. The theoretical calculations show that, at lower energies, $\Delta\sigma_{\text{align}}$ depends appreciably on the coupling with the low-lying levels.

[NUCLEAR REACTIONS $^{59}\vec{\text{Co}}+n$, $E_n=0.8$–20 MeV; measured σ_T and deformation effect $\Delta\sigma_{\text{align}}$; data analyzed by coupled-channel calculations; deduced optical model parameters; no free parameters used in coupling terms.]

I. INTRODUCTION

Experiments with aligned nuclear targets have been performed during the last two decades at several laboratories to study nuclear deformations. The observed effects have generally been grouped under the term "deformation effect," which may be defined as the variation in the yield of a nuclear reaction resulting from the alignment of nonspherical target nuclei bombarded by neutral or charged particles.

The first observation of the deformation effect in fast neutron transmission through an aligned ^{165}Ho target was performed by Wagner *et al.*[1] using 350 keV neutrons. Other neutron transmission experiments on aligned ^{165}Ho were later performed by Marshak *et al.*,[2] Fisher *et al.*,[3] McCarthy *et al.*,[4] Marshak *et al.*,[5] and Fasoli *et al.*,[6] using neutrons of energies ranging from 0.3 to 120 MeV. Further investigations were done employing electrons,[7] protons,[8] α particles,[9] and neutrons[10] as probes and observing the deformation effect in elastic scattering. Analysis of these experimental data produced several interesting results. In particular, it was firmly established that ^{165}Ho in the low-lying states behaves like a rigid rotor with a prolate shape; the value of its deformation parameter was also precisely determined. Furthermore, the interpretation of the giant resonances in the total neutron cross section previously proposed by Peterson[11] was confirmed.[5]

The next nuclide to be investigated was ^{59}Co, whose alignment became possible with the advent of dilution refrigerators. The deformation effect on neutron transmission through a cobalt single crystal with an alignment degree of 16% was measured by Fisher *et al.*[12] at five energies between 1 and 2 MeV and at 15.9 MeV. The results of the experiment clearly confirmed the ^{59}Co deformation, already observed with other techniques. The theoretical analysis of the data performed by a DWBA calculation was complicated by the fact that most of the results were in the energy region between 1 and 2 MeV where the presence of large fluctuations in the total neutron cross section hindered the application of the optical model.

In the present experiment, from which preliminary data were reported in Ref. 13, the observation of the deformation effect in neutron transmission through aligned ^{59}Co was extended over the neutron

energy range from 0.8 to 20 MeV. The target alignment was 34%.

^{59}Co is situated in a region of nuclear masses where nuclei do not exhibit collective rotational spectra. However, atomic spectroscopy experiments[14–16] clearly show that electric quadrupole moments (and in particular that of ^{59}Co) are greater than the single-particle estimates. In addition, the shape of the neutron photonuclear cross section for nuclei in this region, as observed by Fultz *et al.*,[17] Baciu *et al.*,[18] and Alvarez *et al.*,[19] shows some collective effects. Attempts to explain the experimental data on ^{59}Co with theoretical calculations based upon rigid deformation, hydrodynamical, vibrational, and dynamic-collective models have not given fully satisfactory results.[19] This seems to indicate that the nuclear structure of ^{59}Co is more complex than that assumed in these models. Davies, Satchler, Drisko, and Bassel[20] have suggested that the nuclear deformations which correspond to the measured electric quadrupole moments of odd nuclei in regions where the even-even nuclei exhibit vibrational characteristics are due to the interaction between the odd nucleon (or hole) and the vibrational core, which is partially polarized by the nucleon. The lowest energy levels of odd cobalt isotopes have thus been described as originating from the coupling between the nickel vibrational core and a proton hole.[21–25] Although the results of these models are not entirely satisfactory, they are generally successful in predicting the parameters of low-lying excited levels (energies, spins, and parities), spectroscopic factors for direct reactions, and transition probabilities. Following this theoretical line, we have analyzed the data of the present experiment by employing the method outlined by Ford *et al.*,[26] which is essentially an extension of the one introduced by Tamura.[27]

II. THE EXPERIMENT

A. Experimental arrangement and electronic apparatus

The experimental apparatus used for the measurement of the ^{59}Co deformation effect is displayed in Fig. 1. The cobalt single crystal C was aligned by means of the ^{3}He-^{4}He dilution refrigerator R. The neutron beam generated in the neutron source S was collimated and detected by the counter D after transmission through the target. The neutrons were produced by stopping a 4 MeV deuteron beam in a natural lithium target 1 mm thick. Principal contributions came from the reactions (d,n), (d,n'), and $(d,n\alpha\alpha)$ on ^{7}Li having Q values of 10.03, 12.03, and 15.12 MeV, respectively. Some neutrons were also produced by (d,n) reactions on ^{6}Li (isotopic abundance 7%) and on oxygen and carbon which were present as contaminants. A time-of-flight spectrum of the source neutrons is presented in Fig. 2, where the contributions of the various reactions are indicated. The deuteron beam, supplied by the 7 MV CN Van de Graaff accelerator at Legnaro, was pulsed at a frequency of 10^6 Hz with a pulse width of 2 ns FWHM.

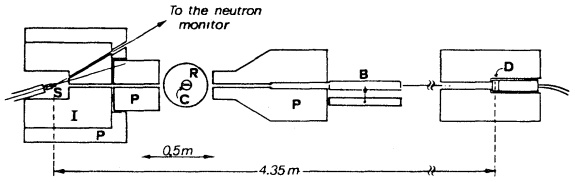

FIG. 1. Experimental apparatus. S, neutron source; P, paraffin screens; I, iron screens; D, neutron detector with a paraffin and $LiCO_3$ screen; B, iron shadow bar; C, cobalt single crystal inside the dilution refrigerator R.

The large mass of the refrigerator and the relatively high intensity and energy of the neutron beam necessitated the use of heavy shielding of iron and paraffin to reduce the neutron background. Two neutron beams, symmetrical with respect to the deuteron beam direction and hence equal in intensity and spectral shape, were defined by means of two narrow holes drilled in the iron block surrounding the neutron source. The first beam passed through the cobalt sample and was detected by the main detector; the second entered the neutron monitor. Both neutron detectors were composed of liquid scintillator NE213, contained in cylindrical glass capsules 5.12 cm wide and 2.56 cm thick and viewed by 56AVP photomultipliers. They were located at identical distances of 4.35 m from the neutron

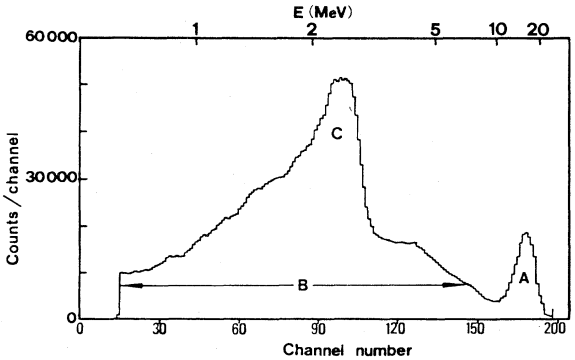

FIG. 2. Time-of-flight and energy spectrum of the incident neutron beam (background subtracted). A, B, and C indicate neutron groups generated as follows: A by the reactions (d,n) and (d,n') on ^{7}Li, B by the reaction $(d,n\alpha\alpha)$ on ^{7}Li, and C by the reactions (d,n) and (d,n') in carbon and oxygen.

source. A conventional time-of-flight technique was used, aided by pulse-shape discrimination, with a neutron detection bias of 0.5 MeV. The time-of-flight spectra of the two neutron detectors were simultaneously recorded by an on-line data acquisition system SADIC (Ref. 28) featuring an HP 2100 computer. The dead time of the counting system was less than 2% and was the same for the two counters. Dead-time correction was therefore unnecessary. The simultaneous recordation of the two time-of-flight spectra permitted "channel-by-channel monitoring," which greatly reduced systematic errors due to fluctuations in the shape of the incident neutron spectrum (e.g., from variation in oxygen and carbon contaminants). The neutron energy was deduced from the time-of-flight over the flight path of 4.35 m. The energy calibration was checked by observing the positions of well-known resonances in the total n-^{12}C neutron cross section. The experimental energy resolution (mainly limited by the 2-ns width of the deuteron pulse) was 1.9% at 1 MeV, 5% at 10 MeV, and 7% at 20 MeV.

B. Aligned cobalt target

It is known that in a hexagonal cobalt single crystal the ^{59}Co nuclei align themselves spontaneously in the direction of the c axis of the crystal at temperatures lower than some tens of mK, even in the absence of an external magnetic field.[29] In this experiment, the ^{59}Co target was composed of two cobalt single crystals having the form of truncated cones, with a total mass of 45 g and a total thickness of 2.370 cm. They were grown in-house using the Czochralski method.[30] For each crystal, the orientation of the c axis was parallel to the geometrical axis of the cone to within a few degrees, as determined by x-ray diffraction methods. The crystals were soft soldered, with the c axes parallel to the neutron beam, inside a small copper block which formed the bottom of the mixing chamber of the refrigerator.

The ^{3}He-^{4}He dilution refrigerator is described in Ref. 31. The lowest temperature obtained in the mixing chamber without the cobalt target was 15 mK. The temperature of the target during the experiment was monitored by carbon resistors calibrated with a cerium-magnesium nitrate thermometer and a ^{60}Co nuclear orientation thermometer[32] soft soldered to the mixing chamber. The average temperature of the target during the experiment was 18.5 mK with variations not exceeding 1 mK.

The nuclear alignment $B_2/B_2(\max)$ of the cobalt single crystal is a function of the temperature and of the hyperfine parameter $H\mu/kI$ (see, for example, Lounasmaa[33]). At the temperature of (18.5 ± 1) mK and with a value 1.07×10^{-2} K for the ^{59}Co hyperfine parameter,[34] one finds $B_2/B_2(\max)=(0.34\pm0.02)$.

C. Experimental procedure

The deformation effect was expected to be small; it was therefore important to minimize all the possible causes of spurious effects. To this end, the cobalt target alignment with respect to the neutron beam was established first by means of a transit and then verified by radiography. Finally, the centering of the neutron beam profile on the target was checked by moving the entire refrigerator at liquid helium temperature in small steps horizontally and vertically. It was estimated that the cobalt target was centered on the neutron beam axis to within a few tenths of a mm.

A source of spurious effects may be due to time drifts of the electronic apparatus. This effect is obviously enhanced when the measurements of the two transmissions (the first through the warm, unaligned target and the second through the cold, aligned target), are separated by the long interval of time (approximately 10 h) required to cool the target from about 1 K to the minimum temperature of 18.5 mK. Errors due to this effect were minimized by adopting the following procedure. The neutron transmissions through the warm (1 K) and cold (18 mK) single crystal cobalt target were compared to the corresponding transmissions through a second polycrystalline cobalt target of identical shape. The comparison was made by moving the entire refrigerator laterally on wheels running on precision rails. The alternating period of a few min was sufficiently short to average out the time drifts of the counting electronics and the deuteron beam pulsing apparatus.

The deformation effect was measured, using this procedure, in a "cold" run, with the target aligned at the temperature of 18.5 mK. The cold run was preceded and followed by "warm" runs at 77 and 1 K (target with zero alignment), respectively. At the end of the experiment the absolute total cobalt neutron cross section was also measured using the same procedure, but with the polycrystalline reference cobalt target removed.

The deformation effect $\Delta\sigma_{\text{align}}(E_i)$ as a function of the incident neutron energy E_i, i being the channel number of the time-of-flight spectrum, was calculated by the formula

$$\Delta\sigma_{\text{align}}(E_i)=\frac{1}{nt}\ln[T_2(E_i)/T_1(E_i)] \ , \qquad (1)$$

where $n=0.896\times10^{23}$ is the number of cobalt nuclei per cm^3 in the target, $t=2.370$ cm is the target thickness, and $T_1(E_i)$ and $T_2(E_i)$ are the neutron transmissions through the aligned cobalt target and

the unaligned reference target, respectively (corrected for the neutron background, which was less than 2%). The time-of-flight interval was divided into 150 channels, each about 2 ns wide; 2 ns also being the approximate time resolution.

D. Experimental results

The results of the measurement are presented in Fig. 3. Figure 3(a) shows the results of the two warm runs, which were equal within errors. For these runs, the average relative difference in transmission between the unaligned single crystal and the polycrystalline reference target was $(6\pm3)\times10^{-4}$. The spurious effects were therefore small in comparison with the deformation effect, shown in Fig. 3(b), which was of the order of a percent or greater over most of the range. The errors indicated in Fig. 3 are statistical. They vary as a function of the neutron energy because of the shape of the incident neutron energy spectrum (Fig. 2). In Fig. 3(b) the six experimental points obtained by Fisher *et al.*[12] are also shown, normalized to the present results by assuming the effect to be proportional to the nuclear alignment (0.34 in the present experiment and 0.16 in Ref. 12). The agreement is remarkably good.

In Fig. 4 the cobalt total neutron cross section

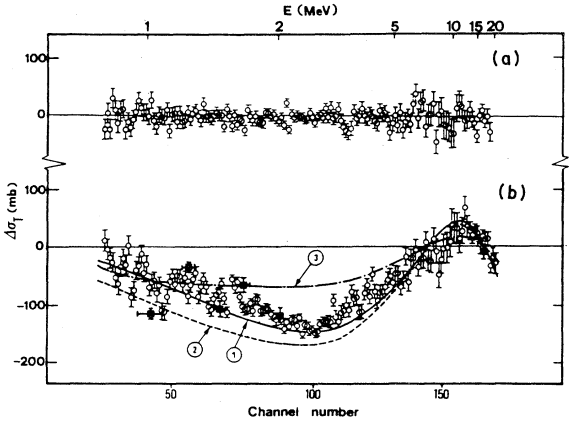

FIG. 3. (a) Difference between the total neutron cross sections of the unaligned ^{59}Co single crystal and the polycrystalline ^{59}Co reference target. (b) Experimental and theoretical deformation effect, $\Delta\sigma_{\text{align}}$, of ^{59}Co as a function of the incident neutron energy. The open circles are the results of the present experiment. The error bars indicate statistical errors only. The full squares are the data of Ref. 12. The curves represent the results of coupled-channel calculations (see text). Curve 1: $\frac{7}{2}^-$, $\frac{9}{2}^-$, $\frac{3}{2}^-$ coupled levels, $\beta_2=0.238$. Curve 2: only $\frac{7}{2}^-$ level, $\beta_2=0.238$. Curve 3: $\frac{7}{2}^-$, $\frac{9}{2}^-$, $\frac{3}{2}^-$ coupled levels, $\beta_2=0.15$.

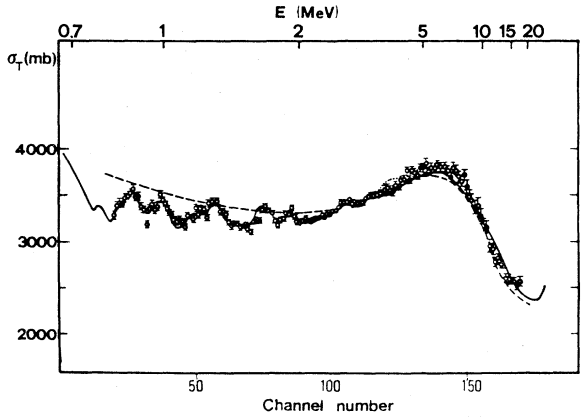

FIG. 4. Experimental and theoretical total neutron cross section of ^{59}Co. The open circles are the data of the present work. The error bars indicate statistical errors only. The solid line represents the averaged data of Ref. 35. The dotted line between about 3 and 6 MeV is a visual fit of the data reported in Ref. 36; above 6 MeV these data are graphically indistinguishable from our data. The dashed line represents the result of the optical model coupled-channel calculations with the parameters given in Table II.

measured in the present experiment is shown, together with data of other authors. The solid line in the figure was obtained by properly averaging, over energy intervals corresponding to our energy resolution, the data obtained with very high resolution and statistical accuracy at Karlsruhe.[35] The dotted line, taken from Ref. 36, represents a visual fit above 3 MeV to data measured by Foster and Glasgow and by Carlson and Barschall. The agreement between the results of the different experiments, particularly below 2 MeV where large fluctuations are apparent, again confirms the validity of the present experimental procedure.

III. THEORETICAL ANALYSIS

A. Coupled-channel optical model for ^{59}Co

As regards the coupled channel optical model calculation, we shall refer to the work of Tamura.[27] The formulae contained therein will later be referred to with the letter *T*. In the coupled-channel optical model calculation, the coupling between scattering states is usually described by the operator *T*-26

$$V_{\text{coupl}}=\sum_{t\lambda} v_\lambda^{(t)}(r)(Q_\lambda^{(t)}\cdot Y_\lambda) \ , \tag{2}$$

where t differentiates terms of different physical character but of the same tensorial rank λ, $v_\lambda^{(t)}(r)$ are form factors deduced from the general form of

the optical potential, and $Q_\lambda^{(t)}$ indicates an operator which operates only on the coordinates of the target nucleus. The matrix elements of V_{coupl} between scattering states of total angular momentum J, resulting from the coupling of a neutron with orbital momentum l, spin s, and total angular momentum j, with states of the target nucleus having angular momentum I (represented as $|ljI\rangle$), can be deduced using a straightforward calculation and are given by

$$\langle ljI \mid V_{\text{coupl}} \mid l'j'I' \rangle = \sum_{t\lambda} v_\lambda^{(t)}(r) \langle I||Q_\lambda^{(t)}||I'\rangle A(ljI,l'j'I',\lambda Js) \quad (3)$$

with the geometrical factor A given by T-28. The physical characteristics of the target nucleus are included in the reduced-matrix elements $\langle I||Q_\lambda^{(t)}||I'\rangle$ which interconnect the low-lying states of the target nucleus.

In the case of ^{59}Co a number of papers[21,23–25,37] have described the low-lying levels in terms of states of the vibration nucleus ^{60}Ni coupled with single particle (or quasiparticle) states of a proton hole. Following the procedure of Refs. 23 and 37, we have described the low-lying states of ^{59}Co as states of a proton hole in the configuration $(1f_{7/2})^{-1}$ coupled to a vibrational harmonic core containing up to a maximum of three quadrupole phonons. The characteristics of the vibrational core were assumed to be those of ^{60}Ni (Ref. 38); in particular the quadrupole phonon energy was assumed to be equal to that of the lowest 2^+ level, namely $\hbar\omega_2 = 1.33$ MeV. In accordance with the data of both Refs. 38 and 39, $\beta_2 = 0.238$ was taken as the value of the deformation. The particle-vibration coupling constant

$$\left\langle 1f_{7/2} \left| r\frac{dV}{dr} \right| 1f_{7/2} \right\rangle$$

was deduced from the wave function calculated with a Saxon-Woods potential including a spin-orbit term[40] and a Coulomb term derived from a uniform spherical charge distribution.[37] Such a description reproduces only approximately the ground-state electric quadrupole moment ($q_{\text{th}} = 0.61$ e b, $q_{\text{exp}} = 0.41 \pm 0.03$ e b), the sequence of the experimental levels, the level energies, and the transition rates $B(E_2)$, as reported in Ref. 41. It is, however, to be pointed out that this description does not contain free parameters. A better reproduction of the experimental data was obtained by Stewart *et al.*[24] by introducing quasihole states coupled with a vibrational anharmonic quadrupole core. The particle-vibration coupling intensity, however, was allowed to vary to obtain the best fit to the experimental data.

In the present description a generic low-lying state of ^{59}Co, characterized by a set of quantum numbers (n,I,M), may be written as

$$|nIM\rangle = \sum_{jN_2R_2} a_{jN_2R_2}^{nI} \, |j,N_2R_2;IM\rangle \ , \quad (4)$$

where j is the spin of the single proton hole, N_2 is the number of quadrupole phonons in the core, R_2 is the core angular momentum, and $a_{jN_2R_2}^{nI}$ are numerical coefficients calculated according to the above scheme[23,37] and listed in Table I.

In the calculation of the reduced-matrix elements $\langle I'||Q_\lambda^{(t)}||I\rangle$, the interaction between the incident particle and the hole was neglected. In this case V_{coupl} reduces to the interaction between the incident neutron and the core, and the expression T-13 may be applied for the form factors $v_\lambda^{(t)}(r)$ and T-31 for the operators $Q_\lambda^{(t)}$. The single proton hole plays the role of core polarizer, without making any contribution to the coupling between scattering states; its contribution to the diagonal part of the scattering is incorporated in the optical potential, whose parameter determination will be described later. Since, according to this view, Q_λ operates on the collective (vibrational) coordinates of the core only, the application of the Wigner-Eckart theorem for a composite system (see, e.g., formula 1A-72, p. 84 of Ref. 42) leads to

$$\langle n'I'||Q_\lambda||nI\rangle = \sum_{jN_2R_2} \sum_{j'N_2'R_2'} a_{jN_2R_2}^{nI} a_{j'N_2'R_2'}^{n'I'} \hat{I}\hat{I}'(-1)^{j+R_2+I'+2} \begin{Bmatrix} j & R_2 & I \\ \lambda & I' & R_2' \end{Bmatrix} \langle N_2'R_2'||Q_\lambda||N_2R_2\rangle \ . \quad (5)$$

The reduced-matrix elements are given by the expressions T-36, T-37, and T-39, and for three-phonon states by the formula 6B-42 of Ref. 43, p. 690.

B. Optical model parameter determination

The potential describing the n-^{59}Co interaction in the optical model coupled-channel formalism is written as

$$V(r,\theta,\phi) = -(V+iW)\frac{1}{1+\exp((r-R)/a)} - 4iW_D \frac{\exp((r-\bar{R})/\bar{a})}{[1+\exp((r-\bar{R})/\bar{a})]^2} - V_{\text{so}}(\bar{\sigma}\cdot\bar{l})\lambda_\pi^2 \frac{1}{ar} \frac{\exp((r-R)/a)}{[1+\exp((r-R)/a)]^2} \quad (6)$$

TABLE I. Expansion coefficients $a^{nI}_{(7/2)N_2R_2}$ [see Eq. (4)] for the first six collective states of ^{59}Co. The corresponding experimental (Ref. 41) and theoretical level energies are also reported.

N_2	R_2 \ n / I^π	1 $\frac{7}{2}^-$	2 $\frac{3}{2}^-$	3 $\frac{9}{2}^-$	4 $\frac{11}{2}^-$	5 $\frac{5}{2}^-$	6 $\frac{7}{2}^-$
0	0	0.6160	0.0	0.0	0.0	0.0	0.6341
1	2	0.6440	0.6739	0.6613	−0.6561	−0.5840	−0.1040
2	0	0.2412	0.0	0.0	0.0	0.0	−0.4194
2	2	−0.2115	0.6140	−0.3792	−0.2665	−0.4516	0.3923
2	4	0.2669	0.2382	0.5474	−0.6081	−0.5079	−0.2269
3	0	−0.0524	0.0	0.0	0.0	0.0	0.1587
3	2	0.1514	0.1590	0.1680	−0.1530	−0.0963	−0.3775
3	3	0.0055	−0.2615	−0.0566	−0.1485	0.3638	−0.0820
3	4	−0.0559	0.1359	−0.2266	0.0649	−0.2155	0.1610
3	6	0.0536	0.0	0.1910	−0.2812	−0.0821	−0.0744
E_{exp} (MeV)		0.0	1.10	1.19	1.46	1.48	1.74
E_{th} (MeV)		0.0	1.23	0.93	1.28	2.15	2.85

where

$$R = R_0\left[1+\sum\alpha_{\lambda\mu}Y_{\lambda\mu}(\theta,\phi)\right] ,$$

$$\bar{R} = \bar{R}_0\left[1+\sum\alpha_{\lambda\mu}Y_{\lambda\mu}(\theta,\phi)\right] ,$$

$$R_0 = r_0 A^{1/3} ,$$

$$\bar{R}_0 = \bar{r}_0 A^{1/3} ,$$

and A is the mass number of the target nucleus. The parameters to be determined from the experimental data are V, W, W_D, V_{so}, r_0, $\bar{r}_0$, a, and $\bar{a}$. The starting set of parameters was taken from the spherical optical model calculation by Fisher *et al.*[44] The parameters V_{so} and W were kept fixed, and equal to those of Ref. 44 (7 and 0 MeV, respectively). The others, including α and β, the coefficients of energy dependence of V and W_D, respectively, were varied to obtain the best fit to the total experimental cross section in the energy interval 0.8–20 MeV.

The number of coupled levels is an important factor in computer time consumption. The calculations were performed by coupling together the first three levels (the $\frac{7}{2}^-$ ground state and the first $\frac{3}{2}^-$ and $\frac{9}{2}^-$ excited states), using complex form factors (*T*-13). The number of partial waves considered in the interaction was determined by the condition that the penetrability coefficients relative to the neglected waves should be smaller than 10^{-5}. The result of the fit is displayed in Fig. 4. The optical model parameters obtained are reported in Table II. In Fig. 5, the angular distributions of the elastically scattered neutrons, calculated with the parameter values of Table II, are compared with experimental data at 1.0,[44] 4.0,[44] 7.05,[45] 9.0,[46] 11.0,[47] and 14.0 (Ref. 44) MeV. The agreement is good at the energies 1.0, 4.0, 7.05, and 14.0 MeV; it is reasonable, though less satisfactory, at 9.0 and 11.0 MeV.

C. Deformation effect calculation

The deformation effect was calculated as the difference between the total cross section of an aligned and an unaligned target. It was therefore necessary to know the populations P_M of magnetic substates M at 18.5 mK, the temperature at which the experiment was performed. The value of P_M, calculated by means of the formulae of Ref. 44, are reported in Table III.

TABLE II. Optical model parameter values for ^{59}Co, obtained from the best fit of the total neutron cross section (see text). It should be noted that $V = V_0 + \alpha E$, $W_D = W_0 + \beta E$, E being the neutron energy in MeV.

V_0 (MeV)	α	W (MeV)	W_0 (MeV)	β	V_{so} (MeV)	r_0 (fm)	a (fm)	$\bar{r}_0$ (fm)	$\bar{a}$ (fm)
49.72	−0.5349	0.0	14.23	0.0068	7.0	1.262	0.6078	1.414	0.222

TABLE III. Magnetic substate populations P_M in the neutron beam direction, for the ^{59}Co aligned target, at the temperature of 18.5 mK.

M	$-\frac{7}{2}$	$-\frac{5}{2}$	$-\frac{3}{2}$	$-\frac{1}{2}$	$\frac{1}{2}$	$\frac{3}{2}$	$\frac{5}{2}$	$\frac{7}{2}$
P_M	0.226	0.131	0.082	0.061	0.061	0.082	0.131	0.226

The results of the calculations for $\Delta\sigma_{\text{align}}$ are shown in Fig. 3(b). Curve 1, corresponding to $\beta_2=0.238$, agrees very well with the experimental data. We have also investigated the importance of the level coupling in the calculation of $\Delta\sigma_{\text{align}}$. It is apparent from curve 2 of Fig. 3(b) that it is necessary to include more than just the ground state alone in the calculation, particularly for neutron energies lower than 4 MeV. The inclusion of the first excited state gave good agreement with the experimental data, and the inclusion of the second excited level did not appreciably improve this agreement. The total cross section, on the other hand, was almost completely insensitive to the inclusion of any levels above the ground state. Figure 6 shows the dependence of $\Delta\sigma_{\text{align}}$ on β_2, the deformation parameter of the vibrational core, for five values of the incident neutron energy. Curve 3 of Fig. 3(b) displays the dependence of $\Delta\sigma_{\text{align}}$ on the incident neutron energy for $\beta_2=0.15$. Both figures indicate that the dependence of $\Delta\sigma_{\text{align}}$ on β_2 is very critical. Using a best-fit procedure, based on the curves of Fig. 6, one obtains $\beta_2=0.224$. This value is not substantially different from 0.238, which corresponds to curve 1 of Fig. 3(b), and lies well within the range of values of β_2 obtained from other experiments.

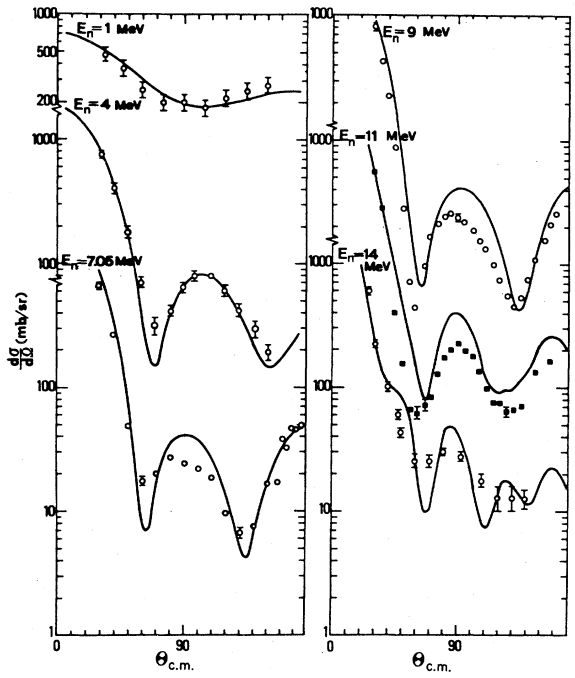

FIG. 5. Experimental and theoretical angular distributions for neutron elastic scattering from ^{59}Co at 1.0 (Ref. 44), 4.0 (Ref. 44), 7.05 (Ref. 45), 9.0 (Ref. 46), 11.0 (Ref. 47), and 14.0 (Ref. 44) MeV. A compound elastic scattering contribution was added at 1.0 MeV as in Ref. 44; a constant contribution of 10 mb/sr was added at 4 MeV.

IV. CONCLUSIONS

The deformation effect in the fast neutron total cross section was measured with an aligned ^{59}Co target having a nuclear alignment $B_2/B_2(\text{max})=0.34$ in the neutron energy interval from 0.8 to 20 MeV. The observed effect varies smoothly with neutron energy, ranging from a value of -5% of the total cross section at 2.5 MeV to $+1\%$ at 10 MeV and then decreasing to -1% at 20 MeV. Below 1.5 MeV, large fluctuations are apparent, similar in position and shape to those present in the total cross section curve. The six energy points measured by Fisher *et al.*[12] are in agreement with the present results.

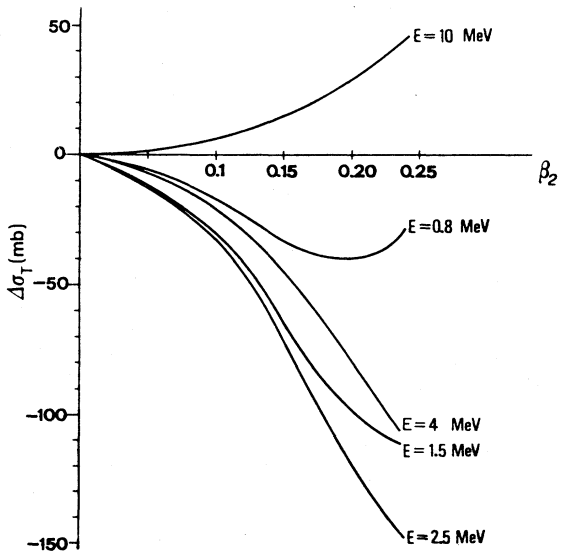

FIG. 6. The deformation effect, $\Delta\sigma_{\text{align}}$, of ^{59}Co as a function of β_2, the deformation parameter of the vibrational core, calculated for five values of the incident neutron energy.

The oscillatory character of the effect recalls a similar feature of the deformation effect on ^{165}Ho observed by McCarthy *et al.*[4] and by Marshak *et al.*[5] which was clearly explained by an optical model calculation as being due to the large prolate deformation of ^{165}Ho. ^{59}Co belongs to a nuclear mass region where rotational spectra, characteristic of large rigid nuclear deformation, are not present. On the other hand, odd nuclei in this region do show large ground state electric quadrupole moments which are evidence of large permanent deformations. In the case of ^{59}Co, we have shown that the deformation effect is adequately explained by a model which couples a ^{60}Ni core to a $(1f_{7/2})$ proton hole with core polarization induced by the proton hole. The coupling with ^{59}Co excited states contributes noticeably to the deformation effect at energies <4 MeV. The core deformation β_2 is consistent with results from other experiments.

ACKNOWLEDGMENTS

We wish to thank L. Badan and G. Bressanini for their continuous and invaluable cooperation during the construction of the cryogenic and electronic apparatus and during the performance of the experiment. Thanks are also due to the staff of the Istituto Nazionale di Física Nucleare (INFN) Laboratory of Legnaro and in particular to R. Preciso and L. Donà of the mechanical workshop where the dilution refrigerator was constructed. Finally we acknowledge the kind cooperation of C. Rossi Alvarez in the use of the data acquisition system SADIC.

[1]R. Wagner, P. D. Miller, T. Tamura, and H. Marshak, Phys. Rev. 139, 29 (1965).
[2]H. Marshak, A. C. B. Richardson, and T. Tamura, Phys. Rev. 150, 996 (1966).
[3]T. R. Fisher, R. S. Safrata, E. G. Shelley, J. McCarthy, S. M. Austin, and R. C. Barrett, Phys. Rev. 157, 1149 (1967).
[4]J. S. McCarthy, T. R. Fisher, E. G. Shelley, R. S. Safrata, and D. Healey, Phys. Rev. Lett. 20, 502 (1968).
[5]H. Marshak, A. Langsford, C. Y. Wong, and T. Tamura, Phys. Rev. Lett. 20, 554 (1968); H. Marshak, A. Langsford, T. Tamura, and C. Y. Wong, Phys. Rev. C 2, 1862 (1970).
[6]U. Fasoli, G. Galeazzi, D. Toniolo, and G. Zago, Lett. Nuovo Cimento 6, 485 (1973).
[7]R. S. Safrata, J. S. McCarthy, W. A. Little, M. R. Yearian, and R. Hofstadter, Phys. Rev. Lett. 18, 667 (1967); F. J. Uhrhane, J. S. McCarthy, and M. R. Yearian, *ibid.* 26, 578 (1971).
[8]T. R. Fisher, S. L. Tabor, and B. A. Watson, Phys. Rev. Lett 27, 1078 (1971).
[9]D. R. Parks, S. L. Tabor, B. B. Triplett, H. T. King, T. R. Fisher, and B. A. Watson, Phys. Rev. Lett. 29, 1264 (1972).
[10]U. Fasoli, G. Galeazzi, D. Toniolo, G. Zago, and R. Zannoni, Nucl. Phys. A284, 282 (1977).
[11]J. M. Peterson, Phys. Rev. 125, 955 (1962).
[12]T. R. Fisher, A. R. Poletti, and B. A. Watson, Phys. Rev. C 8, 1837 (1973).
[13]U. Fasoli, G. Galeazzi, P. Pavan, D. Toniolo, G. Zago, and R. Zannoni, Lett. Nuovo Cimento 27, 207 (1980).
[14]D. von Ehrenstein, Ann. Phys. (Leipzig) 7, 342 (1961).
[15]W. J. Childs and L. S. Goodman, Phys. Rev. 170, 50 (1968).
[16]K. Murakawa, J. Phys. Soc. Jpn. 27, 1690 (1969).
[17]S. C. Fultz, R. L. Bramblett, J. T. Caldwell, N. E. Hansen, and C. P. Jupiter, Phys. Rev. 128, 2345 (1962).
[18]G. Baciu, G. C. Bonazzola, B. Minetti, C. Molino, L. Pasqualini, and G. Piragino, Nucl. Phys. 67, 178 (1965).
[19]R. A. Alvarez, B. L. Berman, D. D. Faul, F. H. Lewis, Jr., and P. Meyer, Phys. Rev. C 20, 128 (1979).
[20]K. T. R. Davies, G. R. Satchler, R. M. Drisko, and R. H. Bassel, Nucl. Phys. 44, 607 (1963).
[21]L. Satpathy and S. C. Gujrathi, Nucl. Phys. A110, 400 (1968).
[22]A. Covello and V. R. Manfredi, Phys. Lett. 34B, 584 (1971).
[23]M. Montagna, Thesis, University of Padua, 1971 (unpublished).
[24]K. W. Stewart, B. Castel, and B. P. Singh, Phys. Rev. C 4, 2131 (1971).
[25]J. M. G. Gomez, Phys. Rev. C 6, 149 (1972).
[26]J. L. C. Ford, Jr., C. Y. Wong, T. Tamura, R. L. Robinson, and P. H. Stelson, Phys. Rev. 158, 1194 (1967).
[27]T. Tamura, Rev. Mod. Phys. 37, 679 (1965).
[28]A. Buscemi, M. De Poli, C. Rossi Alvarez, and R. Zanon, in Proceedings of the 1st European HP-1000 User Conference, 1981, edited by M. Beekman, A Van Putten, and P. Zuidema (Reedbooks, Chertsey, Surrey, England, 1981).
[29]M. A. Grace, C. E. Johnson, N. Kurti, R. G. Scurlock, and R. T. Taylor, Philos. Mag. 4, 948 (1959).
[30]U. Fasoli and P. Pavan, Istituto Nazionale di Física Nucleare Report INFN/TC-80/1, 1980 (unpublished).
[31]U. Fasoli, G. Galeazzi, and D. Toniolo, in *Progress in Refrigeration Science and Technology,* Proceedings of the XVth International Congress of Refrigeration, (1979), edited by the Organizing and Scientific Committee of XVth International Congress of Refrigeration (The International Institute of Refrigeration, Paris, 1980), Vol. 1, p. 101.
[32]Supplied by Oxford Instruments Co., Oxford, England.
[33]O. V. Lounasmaa, *Experimental Principles and Methods below 1 K* (Academic, New York/London, 1974).
[34]D. A. Shirley, in *Hyperfine Structure and Nuclear Radiation,* edited by E. Matthias and D. A. Shirley (North-Holland, Amsterdam, 1968), p. 985.

[35]S. Cierjacks, P. Forti, D. Kopsch, L. Kropp, J. Nebe, and H. Unseld, Kernforschungszentrum Report 1000, 1969, Suppl. 2. (unpublished).
[36]M. D. Goldberg, S. F. Mughabghab, B. A. Magurno, and V. M. May, Brookhaven National Laboratory Report BNL 325, 1966 (unpublished).
[37]A. Covello and V. R. Manfredi, Boll. Soc. Ital. Fis. 79, 90 (1970).
[38]R. L. Auble, Nucl. Data Sheets 28, 103 (1979).
[39]G. Bruge, J. C. Faivre, H. Faraggi, and A. Bussiere, Nucl. Phys. A146, 597 (1970).
[40]K. Bleuler, M. Beiner, and R. de Tourreil, Nuovo Cimento 52B, 45 (1967).
[41]H. J. Kim, Nucl. Data Sheets 17, 485 (1976).
[42]A. Bohr and B. R. Mottelson, *Nuclear Structure* (Benjamin, Reading, Mass., 1969), Vol 1.
[43]A. Bohr and B. R. Mottelson, *Nuclear Structure* (Benjamin, Reading, Mass., 1975), Vol. 2.
[44]T. R. Fisher, H. A. Grench, D. C. Healey, J. S. McCarthy, D. Parks, and R. Whitney, Nucl. Phys. A179, 241 (1973).
[45]E. Ramström and P. Å. Göransson, Nucl. Phys. A284, 461 (1977).
[46]D. E. Velkley, D. W. Glasgow, J. D. Brandenberger, M. T. McEllistrem, J. C. Manthuruthil, and G. P. Poirier, Phys. Rev. C 9, 2181 (1974).
[47]J. C. Ferrer, J. D. Carlson, and J. Rapaport, Nucl. Phys. A275, 325 (1977).